

文章编号: 1006-9941 (2013)04-0479-06

Theoretical Study on Solvent Effect on Cycloaddition Reaction: $\text{HN}_3 + \text{NH}_2\text{CN} \rightarrow 5\text{-AT}$

LAI Wei-peng, LIAN Peng, YU Tao, CHEN Xiao-fang, QIU Shao-jun, CHANG Hai-bo

(Xi'an Modern Chemistry Research Institute, Xi'an 710065, China)

Abstract: Cycloaddition reaction $\text{HN}_3 + \text{NH}_2\text{CN} \rightarrow 5\text{-AT}$ has been theoretically investigated by B3LYP, QCISD and MP2 methods with 6-311 + G^* basis set. The solvent effects on the geometries, reaction path properties, energies, thermodynamic, and kinetic characters in four solvents (carbon tetrachloride, dimethylsulfoxide, acetone, and water) have been studied by using self-consistent reaction field (SCRf) approach with the polarizable continuum model (PCM). Results show that effects of solvent on the geometric characters and reaction path properties are negligible. The equilibrium constant in dimethylsulfoxide solvent is the largest, so the reaction easier occurred spontaneously in dimethylsulfoxide solvent thermodynamically. The rate constant in the solvents is smaller kinetically than that in gas phase, and 300 to 350 K is the most feasible temperature to the reaction.

Key words: physical chemistry; solvent effect; thermodynamics; kinetics; theoretical study; cycloaddition

CLC number: Tj5; O642; O643

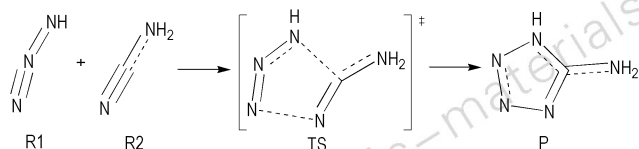
Document code: A

DOI: 10.3969/j.issn.1006-9941.2013.04.015

1 Introduction

Cycloaddition reaction is a pericyclic chemical reaction, in which two or more unsaturated molecules or parts of the same molecule combine with the formation of a cyclic adduct in which there is a net reduction of the bond multiplicity. Cycloadditions are usually described by the backbone size of the participants, which include the [4 + 2] cycloaddition and the [3 + 2] cycloaddition. The [3 + 2] cycloaddition is one of widely used organic chemical reaction, and has been extensively studied for the synthesis of 5-membered heterocycles^[1-2].

5-Amino-1H-tetrazole (5-AT), which was discovered by Thiele in 1893, is one of the most important intermediates for preparation of the high-energy density materials (HEDMs). In the past few years, a number of experiments have been carried out to explore the synthetical methods of 5-AT and derivatives thereof^[3-12]. The reaction of hydrazoic acid (HN_3) combining with the cyanamide (NH_2CN) is a useful method to synthesize 5-AT, which is a typical [3 + 2] cycloaddition (Scheme 1).



Scheme 1 Mechanism of the title reaction

To the best of our knowledge, less theoretical study on the title reaction has been reported^[13-17]. The 1, 3-polar azide anion cycloaddition to nitriles was studied by Jursic, and the calculations agreed with the fact that electron-withdrawing substituents on the nitrile group decreased the activation barrier and facilitated the reaction^[13]. The transition states of both

$\text{HCN} + \text{HN}_3 \rightarrow \text{H}_2\text{CN}_4$ and $\text{HCN} + \text{N}_3^- \rightarrow \text{HCN}_4^-$ reaction were investigated by Chen, and it was found that the latter reaction was more favored than the former one in view of the chemical kinetics and thermodynamics, tetrazole (H_2CN_4) and tetrazolate anion (HCN_4^-) were formed more easily in an alkali environment than in other systems^[14]. The mechanisms of tetrazole formation by addition of azide to nitriles and why the reaction catalyzed by zinc(II) salts were studied by Fahmi. The calculations indicated that coordination of the nitrile to the zinc ion was the dominant factor affecting the catalysis, this coordination substantially lowered the barrier for nucleophilic attack by azide^[15-16]. The mechanism of the azide-nitrile cycloaddition mediated by the dialkyltin oxide-trimethylsilyl azide catalyst system and a new vilsmeier-haack type organocatalyst was investigated by David, and it was shown that as compared to the dialkyltin oxide-trimethylsilyl azide method, the organocatalytic system presented herein had the advantage of higher reactivity, in situ generation from inexpensive materials, and low toxicity^[17]. In this present work, we attempt to perform an intensively theoretical calculation for the solvent effect of the title reaction using B3LYP and high-electron-correlation QCISD and MP2 methods with 6-311 + G^* basis set.

2 Computational Methods

The geometries of all reactants (HN_3 and NH_2CN), transition state, and product (5-AT) have been fully optimized by B3LYP, QCISD, and MP2 methods at 6-311 + G^* level. B3LYP is a DFT method using Becke's three-parameter nonlocal exchange functional with the nonlocal correlation of Lee, Yang, and Parr^[18-19]. QCISD is an extension of configuration interaction that corrects for size-consistency errors in the all singles and double excitation configuration interaction methods^[20-22]. MP2 stands for the second-order Moller Plesset perturbation theory^[23]. 6-311 + G^* is a split-valence triple- ζ polarization basis set augmented with diffuse functions^[23]. The structures and imaginary frequencies of transition states were confirmed by the vibration analysis and the intrinsic reaction coordinate (IRC) method at the same level. The changes of the bond lengths for the reaction as a function of the intrinsic

Received Date: 2012-06-15; **Revised Date:** 2012-10-08

Project Supported: National defence fund(61374)

Biography: LAI Wei-peng(1981 -), female, engaged in energetic materials theoretical research. e-mail: lwpdry@126.com

reaction coordinates were obtained at B3LYP/6-311 + G* level from -3.00 to 3.00 ($\text{amu}^{1/2}$ bohr) using the IRC method with a step size of 0.1 ($\text{amu}^{1/2}$ bohr)^[24-26]. The single-point energies of all stagnation points were calculated at same levels. The statistical thermodynamic method [Eq. (1)] and Eyring transition state theory with Wigner correction [Eq. (2)] were used to determine the thermodynamic functions and rate constants of all reactions from 200 to 450 K.

$$\Delta H = \sum H_{\text{product}} - \sum H_{\text{reactant}}$$

$$\Delta H^\ddagger = H_{\text{TS}} - \sum H_{\text{reactant}}$$

$$\Delta S = \sum S_{\text{product}} - \sum S_{\text{reactant}}$$

$$\Delta S^\ddagger = S_{\text{TS}} - \sum S_{\text{reactant}} \quad (1)$$

$$\Delta G = \Delta H - T\Delta S$$

$$\Delta G^\ddagger = \Delta H^\ddagger - T\Delta S^\ddagger$$

$$K^\ddagger = e^{(-\Delta G^\ddagger/RT)}$$

$$k(T) = g(k_b T/h) \exp(\Delta_r^\ddagger S_m/R - \Delta_r^\ddagger H_m/RT)$$

$$g = 1 + (h\nu^\ddagger/k_b T)^2/24 \quad (2)$$

$$A = g(k_b T/h) \exp(\Delta_r^\ddagger S_m/R)$$

where $k(T)$, reaction rate constant. g , Wigner emendation factor. A , reaction frequency factor. k_b , Boltzmann factor, and h Planck's constant. $\Delta_r^\ddagger H_m$ and $\Delta_r^\ddagger S_m$ are the mole activation enthalpy and mole activation entropy of a reaction system, and ν^\ddagger is the imaginary frequency of a transition state.

To further explore the solvent effects, the above calculations were carried out using self-consistent reaction field (SCRF) approach with the polarizable continuum model (PCM) of the Tomasi's group^[27-32] in four solvents (carbon tetrachloride, dimethylsulfoxide, acetone, and water). All calculations are carried out using the Gaussian 09 software package^[33].

3 Results and discussion

3.1 Geometries

The geometric parameters of the reactants (HN_3 and NH_2CN), products (5-AT), and TS optimized at B3LYP/6-311 + G* level of theory in the gas phase and four different solvents (carbon tetrachloride, acetone, dimethylsulfoxide, and water) are shown in Fig. 1 and Table 1. It is shown that the bond lengths participated in the reaction in TS increases in gas phase and in four solvents compared with those of the corresponding bonds in the reactants. The lengths of C1—N2 bond in TS are longer than that in HN_2CN . The other bond lengths, such as N6—N7 and N7—N8, have similar trend. All above bond lengths are further elongated in 5-AT compared with those in TS. The distance of C1—N8 and N2—N6 have reversed trend in order to form the 5-membered heterocycle. It is also seen that the bond angles participated in the reaction in TS and product are decreased in comparison with those of the corresponding bonds in the reactants.

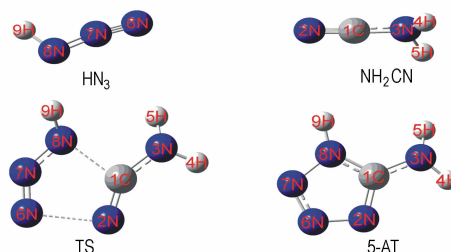


Fig. 1 Optimized geometries of the reactants, transition states (TS), and products

Table 1 Bond parameters of all species optimized at B3LYP/6-311 + G* level of theory (bond length in Å, bond angle in °)

species	bond parameters	gas phase	carbon tetrachloride	acetone	dimethylsulfoxide	water
NH_2CN	C1—N2	1.158	1.158	1.160	1.160	1.161
	N2—C1—N3	177.248	177.196	177.076	177.072	177.076
HN_3	N6—N7	1.131	1.131	1.131	1.131	1.133
	N7—N8	1.239	1.236	1.233	1.233	1.227
	N6—C7—N8	170.867	171.197	171.528	171.554	172.324
TS	C1—N2	1.202	1.197	1.199	1.199	1.196
	N6—N7	1.163	1.160	1.160	1.160	1.159
	N7—N8	1.286	1.275	1.269	1.267	1.281
	C1—N8	1.876	1.913	1.899	1.899	1.914
	N2—N6	2.096	2.124	2.147	2.148	2.118
	N2—C1—N3	145.442	147.172	146.909	147.024	146.899
	N6—C7—N8	132.210	134.260	134.550	134.640	133.989
5-AT	C1—N2	1.319	1.322	1.328	1.327	1.331
	N6—N7	1.280	1.281	1.283	1.283	1.283
	N7—N8	1.367	1.364	1.361	1.360	1.357
	C1—N8	1.350	1.349	1.348	1.348	1.348
	N2—N6	1.363	1.359	1.357	1.357	1.356
	N2—C1—N3	126.279	126.235	126.340	126.345	126.272
	N6—C7—N8	105.833	105.873	105.917	105.894	106.148

3.2 Reaction Path Properties

The variations of the bond lengths with the IRC are shown in Fig. 2. The trends of all bond lengths changing with the intrinsic reaction coordinate s are similar in the gas phase and in four solvents. The bond lengths of C1—N8 and N2—N6 change dramatically with s . In contrast, the bond lengths of all the other bonds change little. As the reaction proceeds from reactants to products, the length of the forming bond C1—N8 and N2—N6 remains minor changed until the intrinsic reaction coordinate reaches $-0.1 \text{ (amu)}^{1/2} \text{ Bohr}$, where they start to fast decrease almost linearly with an increasing s , and the decreasing trend, however, slow after reaching $0.1 \text{ (amu)}^{1/2}$

Bohr. Synchronously, the elongating bond length, such as C1—N3, C1—N2, N6—N7, and N7—N8, increase slowly and almost linearly with s .

It is clear that C1 and N2 are in one molecule (NH_2CN), and N6 and N8 are in another molecule (HN_3) at the starting of cycloaddition. With the reaction proceeding, C1 (or N2) and N8 (or N6) are slowly closed with each other until the distance of C1 (or N2) and N8 (or N6) match the condition of forming a single bond. The elongating bond lengths, however, remain almost unchanged comparing with the forming bond during the reaction due to they are not broke but only changing the kind of bonds.

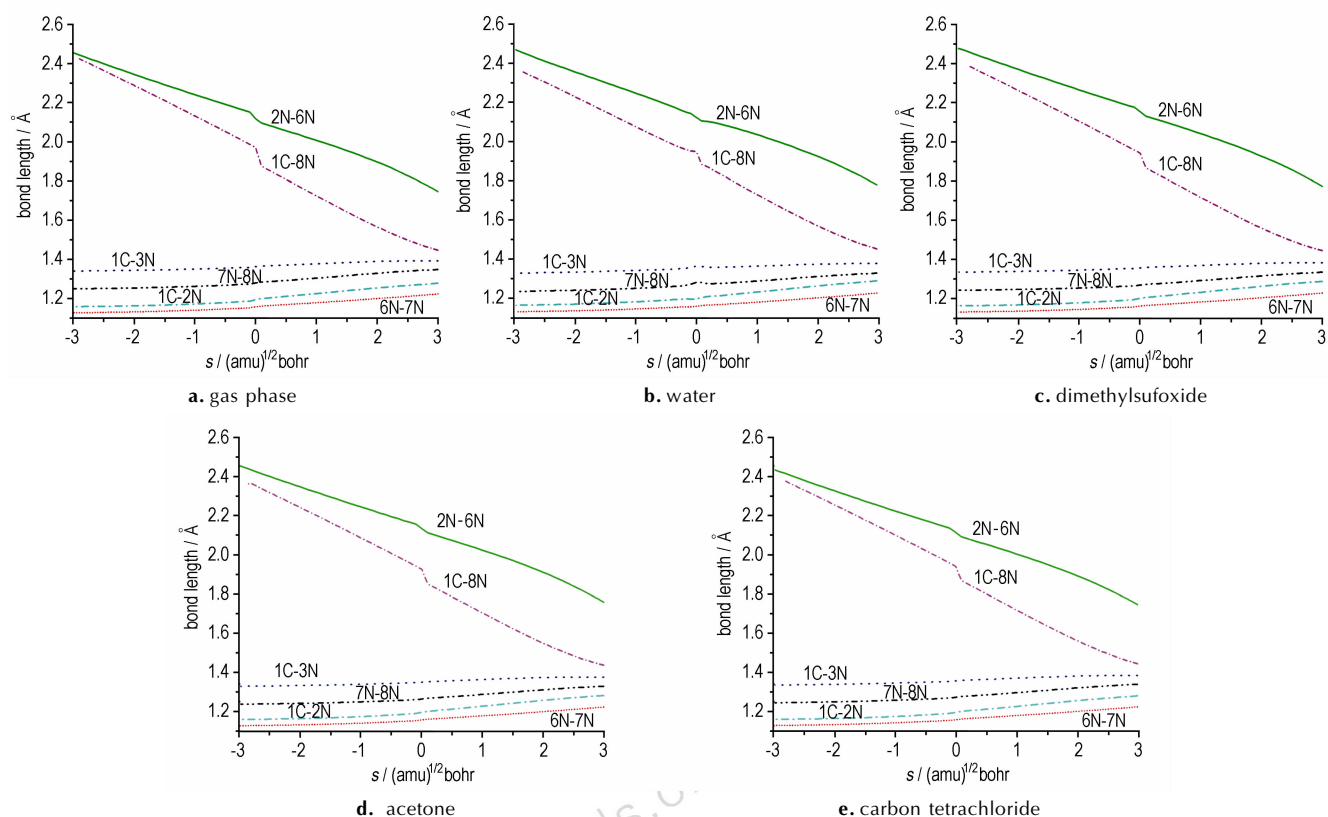


Fig. 2 Changes of the bond lengths (in Å) as a function of the intrinsic reaction coordinate $s \text{ (amu)}^{1/2} \text{ bohr}$ at the B3LYP/6-311 + G* level of theory

3.3 Energies

The zero-point energies (E_{ZPE}) and total energies (E) of all species are calculated by using B3LYP, QCISD, and MP2 method with 6-311 + G* level of theory (Table 2). The potential energies profile of the reaction (corrected by the zero-point energies, emendation factors were 0.96^[34]) are shown in Fig. 3. The activation energy barriers are increased with the solvent polarity. It indicates that the reaction become more difficult in polar solvent than in non-polar solvent.

3.4 Thermodynamics and Kinetics

The gas-phase thermodynamic and kinetic properties of the reaction are calculated from 200 K to 450 K with a step size of 50 K (Table 3). It is shown that ΔH and ΔS of the reaction decreases with increasing of temperature, and the equilibrium

constant (K^\ominus) is similar to them. ΔG of the reaction increase with temperature, and it will become positive when the temperature is higher than 450 K. It indicates that the reaction easily occurs at low temperature, and it will not carry out spontaneously when the temperature exceeds 450 K. According to Van't Hoff equal pressure equation, the equilibrium constants of the reaction is increased with the decreasing of temperature because it is an exothermic reaction. So the reaction has advantage to be taken place at low temperature thermodynamically.

The reaction rate is remarkably increased analyzing from the kinetics, and the reaction is favored with increase of temperature. There is very little change in the reaction frequency factor (A), and A is considered to be a constant, so the reaction belongs to the Arrhenius-type reaction. Synthetically considering the thermodynamics and kinetics, the best reaction temperature is from 300 K to 350 K.

The thermodynamic and kinetic properties of the reaction in gas phase and solvents are shown in Table 4. All reactions are exothermic, entropy-decreasing, and spontaneous, and the equilibrium constants (K^\ominus) are large. Analyzing from the thermodynamics, ΔH and ΔG of the reaction in dimethylsulfoxide solvent are the most negative, and K^\ominus is the largest, so the reaction easier occurred spontaneously in dimethylsulfoxide solvent. Each rate constant in the solvents is smaller than that in gas

phase, so the reaction is favored in gas phase kinetically.

The reaction rate in this calculation is smaller than the experimental data of the [3 + 2] reaction, because catalysts such as Rh, zinc bromide, aluminium chloride, lewis acid are used to accelerate the reaction process, and increase the reaction rate in experiment. The reaction energy barrier can be decreased about 6 ~ 16 kcal/mol by catalysts, and the reaction rate can be increased about $10^3 \sim 10^8$ [15-17].

Table 2 Zero-point energies (E_{ZPE}) and total energies (E) of all species in gas phase and four solvents calculated at B3LYP/6-311 + G*, QCISD/6-311 + G*, and MP2/6-311 + G* level of theory (298.15 K)

	Species	$E_{ZPE}/a.u.$	$E/a.u.$			$\nu^{\#}/cm^{-1}$
			B3LYP/6-311 + G*	QCISD/6-311 + G*	MP2/6-311 + G*	
gas phase	HN ₃	0.021304	-164.8317576	-164.4043082	-164.4089712	525.72i
	NH ₂ CN	0.034197	-148.8286211	-148.4258251	-148.4140825	
	TS	0.058689	-313.6188214	-312.7836098	-312.785651	
	5-AT	0.06376	-313.6965831	-312.8712032	-312.8611076	
carbon tetrachloride	HN ₃	0.021144	-164.8337735	-164.4062717	-164.4111198	529.50i
	NH ₂ CN	0.034087	-148.8327197	-148.4294095	-148.4177948	
	TS	0.058508	-313.6238967	-312.7877901	-312.7898134	
	5-AT	0.063737	-313.7056079	-312.8805669	-312.8708407	
acetone	HN ₃	0.021053	-164.8382109	-164.4106985	-164.4158098	532.62i
	NH ₂ CN	0.033937	-148.8395734	-148.4357437	-148.4242916	
	TS	0.058185	-313.6330062	-312.7959031	-312.7978861	
	5-AT	0.063552	-313.717324	-312.8928486	-312.8836343	
dimethyl sulfoxide	HN ₃	0.021229	-164.8379698	-164.4104475	-164.4155765	533.16i
	NH ₂ CN	0.033938	-148.8394054	-148.4355235	-148.4240816	
	TS	0.05819	-313.6328982	-312.7956627	-312.797575	
	5-AT	0.063554	-313.7179338	-312.893514	-312.8843367	
water	HN ₃	0.020742	-164.8461527	-164.419061	-164.4251235	537.28i
	NH ₂ CN	0.033103	-148.8470399	-148.4421904	-148.4309619	
	TS	0.056499	-313.6453606	-312.8097439	-312.8135068	
	5-AT	0.062262	-313.7295193	-312.9109117	-312.9024068	

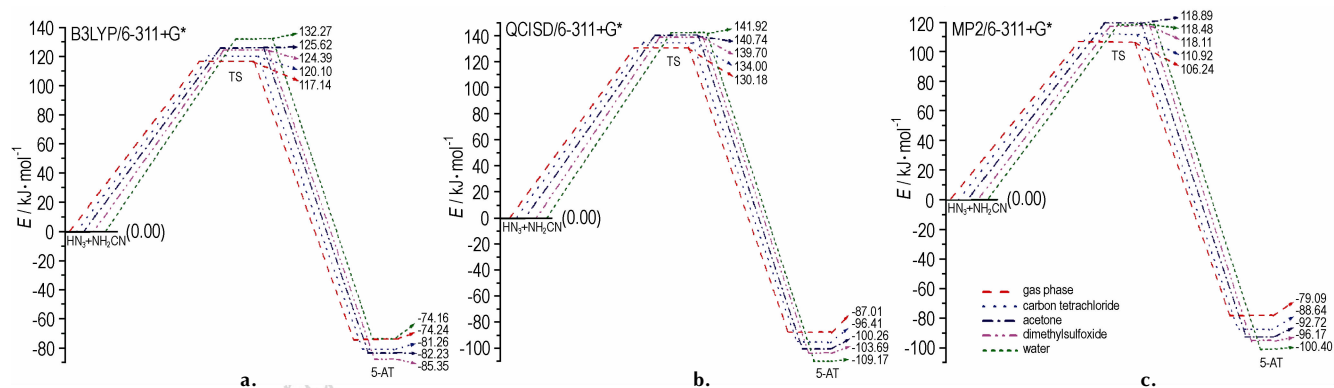


Fig. 3 Potential energy profile of the reaction

Table 3 Calculated thermodynamic and kinetic properties of the reaction in the gas phase at B3LYP/6-311 + G* level (200 K to 450 K)

T /K	ΔH /kJ·mol ⁻¹	ΔH^\ddagger /kJ·mol ⁻¹	ΔS /J·mol ⁻¹ ·K	ΔS^\ddagger /J·mol ⁻¹ ·K ⁻¹	ΔG /kJ·mol ⁻¹	ΔG^\ddagger /kJ·mol ⁻¹	K^\ominus	g	A	$k(T)$ /s ⁻¹
200	-79.05	112.37	-181.86	-166.96	-42.68	145.77	1.40×10^{11}	1.60	1.26×10^4	5.64×10^{-26}
250	-80.06	112.08	-186.39	-168.28	-33.46	154.15	9.82×10^6	1.38	1.17×10^4	4.44×10^{-20}
300	-80.88	111.94	-189.37	-168.82	-24.07	162.58	1.55×10^4	1.27	1.20×10^4	3.88×10^{-16}
350	-81.48	111.90	-191.23	-168.93	-14.55	171.03	148.24	1.20	1.31×10^4	2.60×10^{-13}
400	-81.87	111.95	-192.28	-168.80	-4.96	179.47	4.44	1.15	1.46×10^4	3.50×10^{-11}
450	-82.06	112.08	-192.74	-168.51	4.68	187.91	0.29	1.12	1.65×10^4	1.62×10^{-9}

Table 4 Thermodynamic and kinetic properties of the reaction in gas phase and four solvents at B3LYP/6-311 + G* level of theory (298.15K)

	ΔH /kJ · mol ⁻¹	ΔS /J · mol ⁻¹ · K ⁻¹	ΔG /kJ · mol ⁻¹	K^{\ominus}	ΔH^{\ddagger} /kJ · mol ⁻¹	ΔS^{\ddagger} /J · mol ⁻¹ · K ⁻¹	ΔG^{\ddagger} /kJ · mol ⁻¹	v^{\ddagger} /cm ⁻¹	g	A	$k(T)$
gas phase	-80.87	-189.27	-24.43	1.91×10^4	112.68	-170.26	163.44	525.72i	1.27	1.01×10^4	1.83×10^{-16}
carbon tetrachloride	-88.01	-190.21	-31.30	3.05×10^5	115.66	-169.93	166.33	529.50i	1.27	1.05×10^4	5.72×10^{-17}
acetone	-88.92	-190.04	-32.26	4.49×10^5	121.41	-168.38	171.61	532.62i	1.28	1.27×10^4	6.79×10^{-18}
dimethylsulfoxide	-91.94	-189.42	-35.46	1.63×10^6	120.26	-168.15	170.39	533.16i	1.28	1.30×10^4	1.11×10^{-17}
water	-80.40	-187.88	-24.39	1.87×10^4	128.90	-162.44	177.33	537.28i	1.28	2.60×10^4	6.80×10^{-19}

4 Summary

In this work, we have analyzed the reaction paths, thermodynamic and kinetic properties and solvent effects for the cycloaddition reaction of hydrazoic acid with cyanamide. The B3LYP, QCISD and MP2 methods with 6-311 + G* level of theory are employed to optimize the geometries of all stationary points in gas phase and four solvents.

By analyzing MEP of the reaction, it is found that the regions of occurrence of the cycloaddition reaction in gas phase mainly occurs in the range of $s = -0.1$ to 0.1 (amu)^{1/2} bohr on the MEP of the reaction. The trends of all bond lengths changing with s in the gas phase and four solvents are similar.

The equilibrium constant in dimethylsulfoxide solvent is the largest, so the reaction easier occurred spontaneously in dimethylsulfoxide solvent thermodynamically. Rate constant in the solvents is smaller than that in gas phase kinetically. In gas phase, the reaction is favored with increase of temperature, but has advantage to take place at low temperature thermodynamically, and 300 K to 350 K is the most feasible temperature to the reaction.

References:

- [1] Huisgen R. Kinetics and Mechanism of 1,3-Dipolar Cycloadditions [J]. *Angewandte Chemie International Edition*, 1963, 2 (11): 633–645.
- [2] Huisgen R. 1,3-Dipolar Cycloadditions. Past and Future [J]. *Angewandte Chemie International Edition*, 1963, 2 (10): 565–598.
- [3] Anton H, Hiskey M A, Gerhard H, et al. Azidoformamidinium and Guanidinium 5,5'-Azotetrazolate Salts [J]. *Chem Mater*, 2005, 17(14): 3784–3793.
- [4] Hiskey M A, Goldman N, Stine J R. High-nitrogen energetic materials derived from azotetrazolate [J]. *J Energ Mater*, 1998, 16(2–3): 119–127.
- [5] Hammerl A, Klapötke T M, Nöth H, et al. $[\text{N}_2\text{H}_5]_2^+[\text{N}_4\text{C}-\text{N}=\text{N}-\text{CN}_4]^{2-}$: A new high-nitrogen high-energetic material [J]. *Inorg Chem*, 2001, 40(14): 3570–3575.
- [6] Hiskey M A, Chavez D E, Naud D. 3, 6-Bis(1H-1, 2, 3, 4-tetrazol-5-ylamino)-1, 2, 4, 5-tetrazine or salt thereof: US 6657059 [P], 2003.
- [7] Saikia A, Sivabalan R, Polke B G, et al. Synthesis and characterization of 3, 6-bis(1H-1, 2, 3, 4-tetrazol-5-ylamino)-1, 2, 4, 5-tetrazine (BTATz): Novel high-nitrogen content insensitive high energy material [J]. *J Hazard Mater*, 2009, 170(1): 306–313.
- [8] Sikder A K, Salunke R B, Sikder N. Synthesis, characterization and explosives properties of 7-(1h-1, 2, 4-triazol-3-amino)-4, 6-dinitrobenzofuroxan (TADNB) and 7-(1h-1, 2, 3, 4-tetrazol-5-amino)-4, 6-dinitrobenzofuroxan (TEADNBF) [J]. *J Energ Mater*,

2002, 20(1): 39–51.

- [9] SHENG Di-lun, XU Hou-bao, MA Feng-e. Study on the reaction heat and the optimization of synthesis technology of 5-aminotetrazole [J]. *Chinese Journal of Energetic Materials (Hanneng Cailiao)*, 2005, 13(1): 1–3.
- [10] WANG Hong-she, DU Zhi-ming. Synthesis of 5-aminotetrazole catalyzed by zinc bromide [J]. *Chinese Journal of Energetic Materials (Hanneng Cailiao)*, 2005, 13(6): 368–370.
- [11] XU Song-lin, YANG Shi-qing. Synthesis and properties of high-nitrogen energetic compounds based on azotetrazolate nonmetallic salts [J]. *Chinese Journal of Energetic Materials (Hanneng Cailiao)*, 2006, 14(5): 377–380.
- [12] WANG Yi-hui, DU Zhi-ming, HE Chun-lin, et al. Synthesis and characterization of GZT [J]. *Chinese Journal of Energetic Materials (Hanneng Cailiao)*, 2008, 16(5): 581–584.
- [13] Brabko S J, Zoran Z. Semiempirical and ab initio study of 1, 3-dipolar addition of azide anion to organic cyanides [J]. *Journal of Molecular Structure (Theochem)*, 1994, 312: 11–22.
- [14] Chen C. Theoretical study of synthetic reaction of tetrazole and tetrazolate anion [J]. *Int J Quantum Chem*, 2000, 80: 27–37.
- [15] Fahmi H, Zachary P D, Louis N, et al. Mechanisms of tetrazole formation by addition of azide to nitriles [J]. *J Am Chem Soc*, 2002, 124: 12210–12216.
- [16] Fahmi H, Zachary P D, Louis N, et al. Why is tetrazole formation by addition of azide to organic nitriles catalyzed by zinc(II) salts [J]. *J Am Chem Soc*, 2003, 125: 9983–9987.
- [17] David C, Bernhard G, Kappe C Oliver. Mechanistic Insights on azide-nitrile cycloadditions: on the dialkyltin oxide-trimethylsilyl azide route and a new vilsmeier-haack-type organocatalyst [J]. *J Am Chem Soc*, 2011, 133: 4465–4475.
- [18] Becke A D. Density-functional thermochemistry. III. The role of exact exchange [J]. *J Chem Phys*, 1993, 98(7): 5648–5652.
- [19] Lee C, Yang W, Parr R G. Development of the Colle-Salvetti correlation-energy formula into a functional of the electron density [J]. *Phys Rev B*, 1988, 37: 785–789.
- [20] Pople J A, Martin H G, Krishnan R. Quadratic configuration interaction. A general technique for determining electron correlation energies [J]. *J Chem Phys*, 1987, 87(10): 5968–5975.
- [21] David M, Martin H G. Analytical second derivatives for excited electronic states using the single excitation configuration interaction method: theory and application to benzo[a]pyrene and chalcone [J]. *Molecular Phys*, 1999, 96(10): 1533–1541.
- [22] Martin H G, Rudolph J R, Manabu Q, et al. A double correction to electronic excited states from configuration interaction in the space of single substitutions [J]. *Chem Phys Lett*, 1994, 219(1–2): 21–29.
- [23] Hehre W J, Radom L, Schleyer P V R, et al. *Ab Initio Molecular Orbital Theory* [M]. New York: Wiley & Sons, 1986: 66–80.
- [24] Yang J, Li Q S, Zhang S W. Reaction-path dynamics and theoretical rate constants for the reaction $\text{CH}_4 + \text{O}_3 \rightarrow \text{HOOO} + \text{CH}_3$ [J]. *Int J Quantum Chem*, 2007, 107(10): 1999–2005.

- [25] Li Q S, Zhang Y, Zhang S W. Dual level direct ab initio and density-functional theory dynamics study on the unimolecular decomposition of CH_3OCH_2 radical [J]. *J Phys Chem A*, 2004, 108 (11): 2014 – 2019.
- [26] Zhang Y, Zhang S W, Li Q S. A dual-level ab initio and hybrid density functional theory dynamics study on the unimolecular decomposition reaction $\text{C}_2\text{H}_5\text{O} \rightarrow \text{CH}_2\text{O} + \text{CH}_3$ [J]. *J Comput Chem*, 2004, 25(2): 218 – 226.
- [27] Miertus S, Scrocco E, Tomassi J. Electrostatic interaction of a solute with a continuum. A direct utilization of ab initio molecular potentials for the prevision of solvent effects [J]. *Chem Phys*, 1981, 55: 117 – 129.
- [28] Tomasi J, Persico M. Molecular interactions in solution: an overview of methods based on continuous distributions of the solvent [J]. *Chem Rev*, 1994, 94(7): 2027 – 2094.
- [29] Cammi R, Tomassi J. Remarks on the use of the apparent surface charges (ASC) methods in solvation problems: Iterative versus matrix-inversion procedures and the renormalization of the apparent charges [J]. *J Comput Chem*, 1995, 16(12): 1449 – 1458.
- [30] Cossi M, Barone V, Cammi R, et al. Ab initio study of solvated molecules: a new implementation of the polarizable continuum model [J]. *Chem Phys Lett*, 1996, 255(4 – 6): 327 – 335.
- [31] Cancès M T, Mennuncci V, Tomasi J. A new integral equation formalism for the polarizable continuum model: Theoretical background and applications to isotropic and anisotropic dielectrics [J]. *J Chem Phys*, 1997, 107(8): 3032 – 3041.
- [32] Barone V, Cossi M, Tomasi J. Geometry optimization of molecular structures in solution by the polarizable continuum model [J]. *J Comput Chem*, 1998, 19(4): 404 – 417.
- [33] Frisch M J, Trucks G W, Schlegel H B, et al. Gaussian 09 [CP], Gaussian, Inc Wallingford, CT, 2009.
- [34] Scott A P, Radom L. Harmonic vibrational frequencies: An evaluation of hartree-fock, moller-pleeset, quadratic configuration interaction, density functional theory and semiempirical scale factors [J]. *J Phys Chem*, 1996, 100: 16502 – 16513.

溶剂对环加成反应 $\text{HN}_3 + \text{NH}_2\text{CN} \rightarrow 5\text{-AT}$ 影响的理论研究

来蔚鹏, 廉鹏, 尉涛, 陈晓芳, 邱少君, 常海波

(西安近代化学研究所, 陕西 西安 710065)

摘要: 采用 B3LYP、QCISD、MP2 方法在 6-311 + G* 基组水平上对 $\text{HN}_3 + \text{NH}_2\text{CN} \rightarrow 5\text{-AT}$ 的环加成反应进行了研究, 用气相条件下的计算方法结合 SCRF/PCM 模型对四氯化碳、丙酮、二甲亚砜、水四种不同溶剂下的反应性能进行计算, 探讨了溶剂对反应的影响。结果表明, 溶剂的极性对反应的影响不明显, 从热力学角度考虑: 反应在二甲亚砜溶剂中的平衡常数最大, 说明反应在二甲亚砜溶剂中最容易自发进行; 从动力学角度考虑: 反应在各种溶剂中的速率常数均小于其在气相条件下的速率常数, 说明反应在气相条件下更具有动力学优势。300 ~ 350 K 是该反应的适宜温度。

关键词: 物理化学; 溶剂影响; 热力学; 动力学; 理论研究; 环加成

中图分类号: TJ5; O642; O643

文献标识码: A

DOI: 10.3969/j.issn.1006-9941.2013.04.015